A Colorimetric Analysis of Skin-Tone Sampling Density in the ANSI/IES TM-30-24 Color Evaluation Sample Set

Arpan Guha * , Yurika Fuchise , Andrew Giberson , Lincoln Garrett

Posted Date: 29 May 2026

doi: 10.20944/preprints202605.2042.v1

Keywords: color rendition; TM-30; CAM02-UCS; skin tone; Color Evaluation Samples

 doi:10.20944/preprints202605.2042.v1

Article

A Colorimetric Analysis of Skin-Tone Sampling Density in the ANSI/IES TM-30-24 Color Evaluation Sample Set

Arpan Guha *, Yurika Fuchise, Andrew Giberson and Lincoln Garrett

University of Cincinnati

* Correspondence: guhaan@ucmail.uc.edu

Abstract

ANSI/IES TM-30-24 uses 99 Color Evaluation Samples (CES) selected to provide broad, approximately uniform sampling of object-color space for evaluating color rendition in built environments. Although TM-30 is not intended as a dedicated skin-tone fidelity assessment method, the standard designates two CES, #15 and #18, as skin-tone samples. This study examines how this sampling structure intersects the color space region occupied by measured human skin tones. The analysis used 100 skin reflectance spectra from two independent datasets grouped into five lightness-based categories from Very Light to Very Dark. CAM02-UCS coordinates were computed under D65 using TM-30-specified viewing conditions, and Euclidean nearest-neighbor distances (ΔE′) to the 99 CES were calculated. In both datasets, the Very Dark category showed substantially larger nearest-CES distances than the Very Light category. In the ISSA dataset, Very Dark samples had a mean distance of 8.13 ± 2.17, compared with 3.99 ± 0.59 for Very Light samples. In the CIE dataset, the corresponding values were 7.96 ± 0.94 and 4.24 ± 0.85. Across the combined dataset, Very Dark samples were approximately 95% farther from their nearest CES than Very Light samples. The designated skin CES, #15 and #18, served as nearest neighbors for 51 of 100 samples, primarily in the Very Light, Light, and Medium categories. These findings provide a structural map of how measured skin tones relate to the TM-30 CES set and clarify the role of CES #15 and #18 within the broader skin-tone region.

Keywords: color rendition; TM-30; CAM02-UCS; skin tone; Color Evaluation Samples

1. Introduction

Color rendition describes how a light source affects the appearance of object colors relative to a reference illuminant, and it is central to lighting quality in residential, commercial, healthcare, retail, and institutional environments. ANSI/IES TM-30-24 is the current IES method for evaluating color rendition and uses 99 Color Evaluation Samples (CES) to calculate the Fidelity Index (R_f), Gamut Index (R_g), and related descriptors of color rendition (ANSI/IES TM-30-24, 2024). The method represents a substantial advance over earlier color rendering metrics because it uses a larger sample set, a modern color appearance model, and separate descriptors of fidelity and gamut effects (David et al., 2015). TM-30 calculations are performed in CAM02-UCS, a uniform color space derived from CIECAM02, using specified observer, reference illuminant, and viewing-condition parameters (Luo et al., 2006; Fairchild, 2013; ANSI/IES TM-30-24, 2024). It is important to note that the 99 CES were not selected to serve as a skin-tone database. They were developed to support general color rendition evaluation across a broad range of object spectral reflectance properties encountered in built environments (David et al., 2015; ANSI/IES TM-30-24, 2024). Within that broader framework, TM-30-24 designates two samples, CES #15 and CES #18, as skin-tone samples (ANSI/IES TM-30-24, 2024).

Skin-tone rendering remains relevant because people are frequently viewed under electric light, and prior studies have shown that spectral power distribution and lighting conditions can affect

 doi:10.20944/preprints202605.2042.v1

judgments of skin, complexion, and facial appearance (Veitch et al., 2013; He et al., 2016; Yano and Hashimoto, 2015). Compared to the full range of object colors and spectra, skin reflectance occupies a relatively narrow chromatic region but spans a broad lightness range shaped by melanin, hemoglobin, carotene, and tissue scattering. (Zonios et al., 2001; Jablonski and Chaplin, 2017; Xiao et al., 2017; Del Bino et al., 2018). This combination makes skin tones a useful case for examining local sampling density within a general-purpose color rendition sample set.

Since TM-30 calculations are based on the 99 CES, the local distribution of those samples determines how densely different regions of the color space are represented. A sample set can be well suited for broad, gamut-wide evaluation while still exhibiting different local density within a visually important sub-region. Characterizing that structure is therefore useful before asking whether metric outputs are sensitive to skin-tone rendering under specific light-source spectra. In this context, skin tones provide a focused case for examining how a general-purpose color rendition sample set intersects a constrained but practically important region of object-color space.

To the authors' knowledge, no prior study has directly characterized the distribution of measured skin reflectance spectra relative to the TM-30 CES set in CAM02-UCS color space. The study therefore addresses a specific structural question: how are measured human skin tones positioned relative to the two designated skin CES and to the broader 99-sample CES set? To answer this question, 100 measured skin reflectance spectra from two independent datasets, the International Skin Spectra Archive and the CIE skin-color database, were grouped into five lightness-based categories from Very Light to Very Dark (Xiao et al., 2017; Lu et al., 2025). For each sample, CAM02-UCS coordinates were calculated under D65 using TM-30-specified viewing conditions, and the Euclidean distance to the nearest CES was computed. The objectives were to identify which CES serve as nearest neighbors to measured skin samples, quantify nearest-neighbor distance as an indicator of local CES sampling density, compare results across the two datasets, and determine whether sampling-density patterns differ across skin-tone lightness categories. These analyses do not establish perceptual adequacy or rendering quality under specific illuminants; they characterize the colorimetric structure of the CES set relative to measured skin tones.

2. Methods

A colorimetric nearest-neighbor analysis was utilized to quantify local CES sampling density within the skin-tone region. Measured skin reflectance spectra from two independent datasets were grouped into five CIELAB L^*-based lightness categories and transformed into CAM02-UCS under D65 using TM-30-specified viewing conditions. For each skin sample, the nearest TM-30 CES was identified using Euclidean distance in CAM02-UCS ($\Delta E'$). CIEDE2000 color differences (ΔE_{00}) were also calculated as a robustness check. The analysis pipeline is shown in Figure 1.

2.1. Skin Tone Datasets and Categorization

Two independent spectral skin-tone datasets were used: the International Skin Spectra Archive (ISSA) and the CIE skin-color database (Xiao et al., 2017; Lu et al., 2025). From each dataset, 50 spectra were selected, yielding 100 total skin reflectance spectra. Samples were stratified into five lightness-based categories, with 10 samples per category per dataset: Very Light, Light, Medium, Dark, and Very Dark. The balanced n = 10 per category design was used to support category-level comparison across the lightness range; inferential tests were therefore interpreted with emphasis on effect size and replication across the two independent datasets.

The CIE skin-color database includes calibrated measurements from multiple population groups and body locations, including the forehead, cheek, back of hand, and inner forearm (Xiao et al., 2017). ISSA provides a larger multicultural archive of skin spectral and colorimetric measurements collected across multiple institutions and body locations (Lu et al., 2025). Where available, spectra were selected from facial measurement sites because face appearance is a central concern in people-centered lighting applications. This choice aligned the sample selection with scenarios in which

 doi:10.20944/preprints202605.2042.v1

complexion and visible facial color shifts under electric light are relevant perceptual outcomes (Kiritani et al., 2017; Okuda and Okajima, 2019).

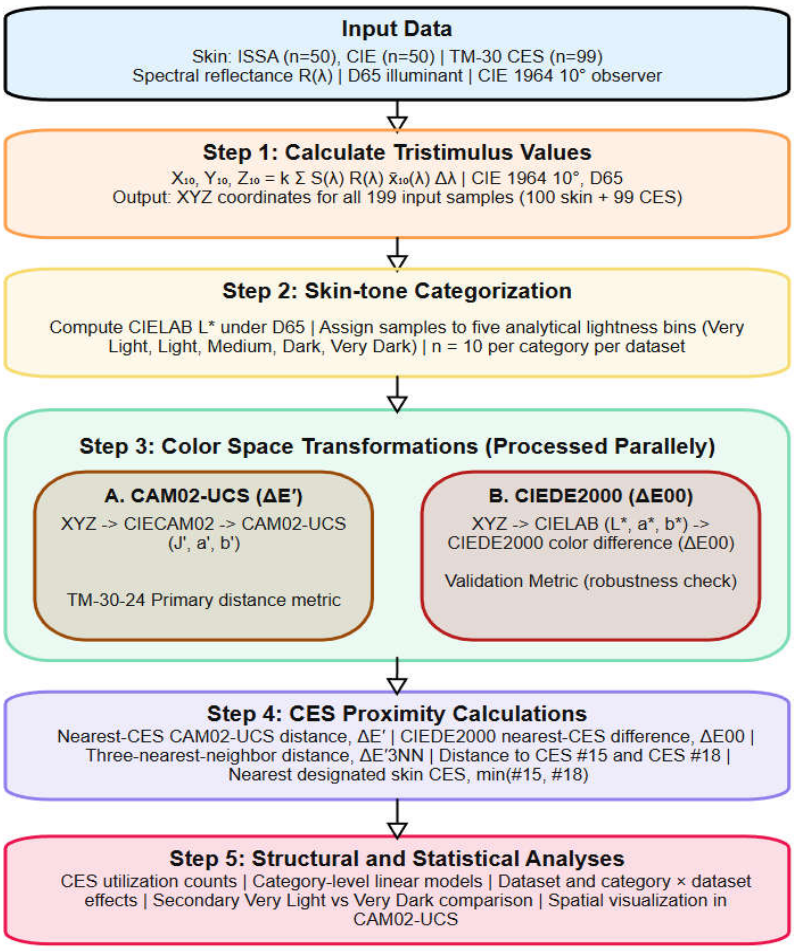

Figure 1. Analysis pipeline for computing nearest-neighbor distances between selected skin-tone spectra and the TM-30-24 CES set.

Skin-tone categories were defined using CIELAB L^* values computed under CIE D65 using the CIE 1964 10° Standard Observer. L^* was used because it provides a direct measure of perceptual lightness and is widely used in skin-color measurement and pigmentation studies (Chardon et al., 1991; Weatherall and Coombs, 1992; Del Bino et al., 2018). The category boundaries were:

- Very Light: $L^* \geq 70$
- Light: $60 \leq L^* < 70$
- Medium: $45 \leq L^* < 60$
- Dark: $35 \leq L^* < 45$
- Very Dark: $L^* < 35$

It must be noted that these categories were used as analytical bins (and not as fixed biological or demographic classes). Skin color varies continuously across individuals and body sites, and alternative systems, including the Individual Typology Angle, incorporate both L^* and b^* values (Chardon et al., 1991; Del Bino et al., 2018). The L^*-based grouping was selected because the analysis focuses on whether nearest-CES distance changes systematically with skin-tone lightness.

2.2. TM-30 CES and Tristimulus Values Computation

The 99 TM-30 CES were obtained from the official ANSI/IES TM-30-24 spectral reflectance data. For each CES and each skin reflectance spectrum, CIE XYZ tristimulus values were calculated under

 doi:10.20944/preprints202605.2042.v1

CIE D65 using the CIE 1964 10° Standard Observer. Calculations followed the standard colorimetric formulation:

$$X_{10} = k \sum S(\lambda)R(\lambda)\bar{x}^{10}(\lambda)\Delta\lambda \quad (1)$$

$$Y_{10} = k \sum S(\lambda)R(\lambda)\bar{y}^{10}(\lambda)\Delta\lambda \quad (2)$$

$$Z_{10} = k \sum S(\lambda)R(\lambda)\bar{z}^{10}(\lambda)\Delta\lambda \quad (3)$$

where k is the normalizing constant calculated using:

$$k = \frac{100}{\sum S(\lambda)\bar{y}^{10}(\lambda)\Delta\lambda} \quad (4)$$

where S(λ) is the D65 spectral power distribution, R(λ) is the sample's spectral reflectance, and $\bar{x}_{10}(\lambda)$, $\bar{y}_{10}(\lambda)$, $\bar{z}_{10}(\lambda)$ are the CIE 1964 10° color matching functions. The summation covered 380-780 nm at 1 nm intervals. The same procedure was applied to the skin spectra and the CES so that all samples entered the CAM02-UCS transformation from a common colorimetric basis (ANSI/IES TM-30-24, 2024).

2.3. CAM02-UCS Color Appearance Pipeline

Following TM-30-24 specifications, color appearance coordinates were calculated using CIECAM02 with the following viewing conditions:

- Adapting field luminance (L_A) = 100 cd/m²
- Background luminance (Y_b) = 20 cd/m²
- Surround parameters: F = 1, c = 0.69, N_c = 1 (Average surround)
- Degree of adaptation: D = 1 (complete adaptation)
- White point: CIE D65 (XYZ = [95.047, 100.000, 108.883])

These parameters match the TM-30-24 calculation procedure and were applied identically to the skin spectra and the 99 CES (ANSI/IES TM-30-24, 2024). Tristimulus values were transformed through CIECAM02 to obtain lightness (J), colorfulness (M), and hue angle (h). These appearance correlates were then converted to CAM02-UCS coordinates using the Luo et al. (2006) transformation:

$$J' = \frac{1.7\,J}{(1 + 0.007\,J)} \quad (5)$$

$$M' = \left(\frac{1}{0.0228}\right)\ln(1 + 0.0228\,M) \quad (6)$$

$$a' = M'\cos\left(h\frac{\pi}{180}\right) \quad (7)$$

$$b' = M'\sin\left(h\frac{\pi}{180}\right) \quad (8)$$

where J′ represents lightness, and a′ and b′ represent the red-green and yellow-blue opponent dimensions, respectively. The resulting three-dimensional CAM02-UCS coordinates provided the basis for calculating Euclidean nearest-neighbor distances (between each skin-tone sample and the TM-30 CES set.

2.4. Nearest-Neighbor Analysis

Nearest-neighbor distance was used to characterize local CES sampling density relative to measured skin-tone locations in CAM02-UCS. In a uniformly sampled color space, points located in denser regions of the sample set are expected to have smaller nearest-neighbor distances than points located in sparser regions. This relationship provides the basis for using nearest-neighbor ΔE′ as an indicator of local CES sampling density. Two additional structural measures were calculated to test whether the observed pattern depended on the single closest CES. First, a three-nearest-neighbor distance ($\Delta E'_{3NN}$) was calculated for each skin sample as the mean CAM02-UCS distance to the three closest CES. This k-nearest-neighbor approach (with k = 3), provides a broader local estimate of CES proximity while avoiding the need to define an arbitrary fixed-radius threshold. Second, because TM-30-24 designates CES #15 and CES #18 as skin-tone samples, distances from each measured skin

 doi:10.20944/preprints202605.2042.v1

sample to CES #15 and CES #18 were calculated directly. The smaller of these two distances was retained as the distance to the nearest designated skin CES. This analysis characterized how the measured skin-tone categories relate specifically to the two CES identified as skin samples in TM-30-24.

For the primary nearest-neighbor analysis, the Euclidean distance from each of the 100 skin-tone samples to each of the 99 TM-30 CES was calculated using:

$$\Delta E' = \sqrt{(J'_{\text{sample}} - J'_{CES})^2 + (a'_{\text{sample}} - a'_{CES})^2 + (b'_{\text{sample}} - b'_{CES})^2} \quad (9)$$

where J′, a′, and b′ are the CAM02-UCS coordinates of the skin sample and CES, respectively. The smallest distance was retained as the nearest-neighbor distance (ΔE′) for that skin sample, and the corresponding CES was recorded as its nearest neighbor. Smaller ΔE′ values indicate that a skin sample is closer to at least one CES in CAM02-UCS under D65, whereas larger values indicate lower local sampling density near that sample. Category-level means were then compared across the five skin-tone lightness groups.

It is important to distinguish this analysis from a color rendering fidelity study. Nearest-neighbor distance in CAM02-UCS quantifies colorimetric proximity under the reference illuminant only. It does not imply spectral similarity between a skin sample and its nearest CES, nor does it predict how either sample will respond under a test illuminant. Two samples may be close in color space under D65 yet have different spectral reflectance functions, leading to different color shifts under light sources with varying spectrums. The nearest-neighbor metric therefore characterizes CES sampling density relative to skin-tone locations, not skin-tone rendering fidelity.

2.5. CIEDE2000 Robustness Check

CIEDE2000 was used as a complementary robustness check because it is a perceptually weighted CIELAB color-difference formula (ΔE_{00}) developed to improve agreement between computed and perceived color differences relative to earlier CIELAB-based formulations (Luo et al., 2001; He et al., 2022). The goal was to test whether the category-level nearest-neighbor pattern persisted under a color-difference formulation with stronger perceptual grounding rather than establishing perceptual thresholds for skin-tone appearance. Skin samples and CES were represented in CIELAB under D65 using the CIE 1964 10° Standard Observer, and CIEDE2000 distances were calculated between each skin sample and each CES using:

$$\Delta E_{00} = \sqrt{\left(\frac{\Delta L'}{k_L S_L}\right)^2 + \left(\frac{\Delta C'}{k_C S_C}\right)^2 + \left(\frac{\Delta H'}{k_H S_H}\right)^2 + R_T \left(\frac{\Delta C'}{k_C S_C}\right)\left(\frac{\Delta H'}{k_H S_H}\right)} \quad (10)$$

where ΔL′, ΔC′, and ΔH′ represent differences in lightness, chroma, and hue, respectively. The weighting functions S_L, S_C, and S_H account for perceptual non-uniformities, k_L, k_C, and k_H are parametric factors (set to 1 for reference conditions), and R_T is a rotation function that corrects for the interaction between chroma and hue differences in the blue region. For each skin sample, the CES with minimum ΔE_{00} value was recorded. These results were compared with the CAM02-UCS nearest-neighbor results to assess whether category-level patterns were consistent across color-difference formulations.

2.6. Statistical Analysis

Descriptive statistics were calculated for ΔE′, ΔE_{00}, $\Delta E'_{3NN}$, and distance to the nearest designated skin CES by dataset and skin-tone category. Since the study objective was to determine whether CES sampling density differed across the full skin-tone lightness range, the primary inferential analysis used linear models instead of relying only on pairwise category comparisons. Separate models were fitted for ΔE′, ΔE_{00}, and the mean $\Delta E'_{3NN}$ with skin-tone category, dataset, and the category × dataset interaction as predictors. The model takes the following form:

$$Y_{ij} = \beta_0 + \beta_1 Category_i + \beta_2 Dataset_j + \beta_3 (Category_i \times Dataset_j) + \varepsilon_{ij} \quad (11)$$

where Y_{ij} represents either ΔE′, ΔE_{00}, or $\Delta E'_{3NN}$ depending on the model. Skin-tone category was treated as a categorical predictor because the groups were defined as analytical lightness bins and

 doi:10.20944/preprints202605.2042.v1

not continuous measurements. Dataset was included to test whether the pattern differed between the ISSA and CIE skin datasets. Linear model effects were summarized using ANOVA-style F tests, degrees of freedom, p-values, and partial eta squared (η_p^2).

To aid interpretation of the category effect, the Very Light and Very Dark categories were also compared directly. This comparison summarized the largest lightness-range separation and was treated as secondary to the all-category linear models. Independent-samples t-tests were used to summarize this contrast within each dataset and for the combined dataset. These comparisons were interpreted as secondary to the all-category linear models. Effect sizes were reported using Cohen's *d*, calculated as:

$$d = \frac{\mu_1 - \mu_2}{\left(\sqrt{\frac{\sigma_1^2 + \sigma_2^2}{2}}\right)} \quad (12)$$

where μ and σ represent means and standard deviations of the two groups. CES utilization patterns were summarized by counting how often each CES served as the nearest neighbor within each dataset and skin-tone category.

3. Results

3.1. ISSA Dataset

The ISSA dataset showed a clear contrast between the lightest and darkest skin-tone categories (Table 1). Very Light samples had the lowest mean distance to the TM-30 CES set, with a mean $\Delta E'$ of 3.99 ± 0.59, while Very Dark samples had the highest mean distance $\Delta E'$ = 8.13 ± 2.17. This corresponds to an approximately 104% increase from the Very Light to Very Dark category. The same pattern was observed using CIEDE2000, with mean ΔE_{00} increasing from 3.95 ± 0.77 for Very Light samples to 7.68 ± 1.65 for Very Dark samples.

Nearest-neighbor assignments also varied by category. CES #15 and #18 serve as nearest neighbors primarily for Very Light, Light, and Medium samples. Dark and Very Dark samples more often mapped to CES without skin designation.

Table 1. Nearest-neighbor color differences and most frequent CES assignments for the ISSA dataset (n = 50).

Category	n	$\Delta E'$ Mean ± SD	ΔE_{00} Mean ± SD	Most Frequently mapped CES
Very Light	10	3.99 ± 0.59	3.95 ± 0.77	#15, #14
Light	10	4.72 ± 1.69	4.46 ± 1.59	#15
Medium	10	5.02 ± 2.40	4.83 ± 2.27	#18, #15, #17
Dark	10	6.40 ± 1.07	5.81 ± 1.64	#13, #16, #39
Very Dark	10	8.13 ± 2.17	7.68 ± 1.65	#3, #9, #13

3.2. CIE Dataset

The CIE dataset showed a similar category-level pattern (Table 2). Very Light samples had a mean nearest-neighbor distance of $\Delta E'$ = 4.24 ± 0.85, while Very Dark samples had the highest mean distance, with $\Delta E'$ = 7.96 ± 0.94. This corresponds to an approximately 88% increase from the Very Light to Very Dark category. CIEDE2000 distances followed the same general pattern, increasing from 4.47 ± 1.20 for Very Light samples to 7.83 ± 1.32 for Very Dark samples. The intermediate categories were not strictly monotonic in the CIE dataset, with Medium samples showing a lower mean $\Delta E'$ than Light samples; however, the primary Very Light-to-Very Dark contrast remained consistent with the ISSA results.

 doi:10.20944/preprints202605.2042.v1

Nearest-neighbor assignments were also consistent with the ISSA results. Very Light and Light samples most often mapped to CES #15, with CES #14 also appearing for Very Light samples. Medium samples mapped most frequently to CES #18, #15, and #17. Dark and Very Dark samples more often mapped to non-designated skin CES, including #13, #16, #17, #3, and #9.

Table 2. Nearest-neighbor color differences (ΔE′ and ΔE00) across five skin tone categories for the CIE dataset (n=50).

Category	n	ΔE′ Mean ± SD	ΔE_{00} Mean ± SD	Most Frequently Mapped CES
Very Light	10	4.24 ± 0.85	4.47 ± 1.20	#15, #14
Light	10	5.71 ± 1.78	5.05 ± 1.63	#15
Medium	10	4.87 ± 2.01	4.62 ± 1.71	#18, #15, #17
Dark	10	6.35 ± 1.09	5.41 ± 0.98	#13, #16, #17
Very Dark	10	7.96 ± 0.94	7.83 ± 1.32	#3, #9, #13

Figure 2 summarizes the distribution of CAM02-UCS nearest-neighbor distances across the five skin-tone categories for both datasets.

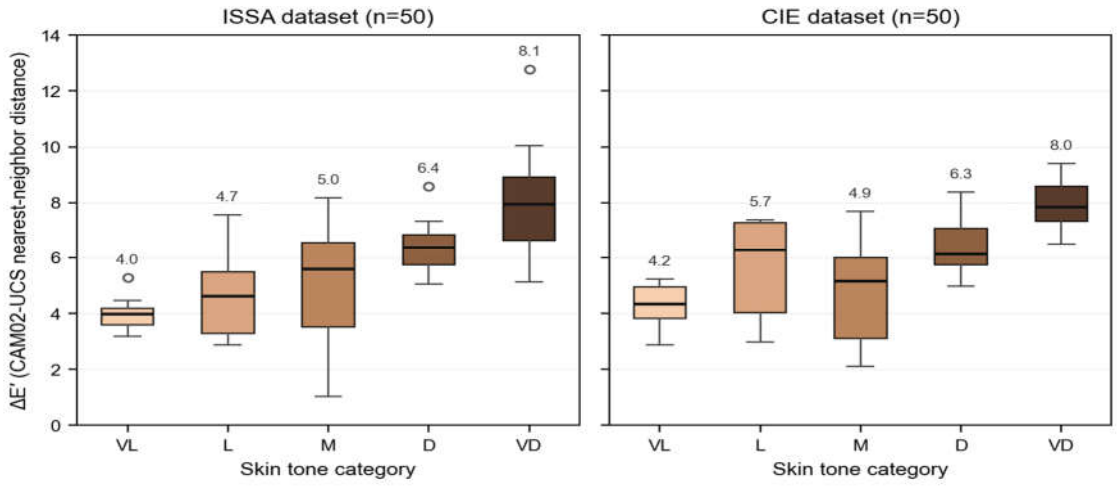

Figure 2. Distribution of CAM02-UCS color differences (ΔE') by skin tone category across the sampled databases.

3.3. Category-Level Model Results and Combined Dataset Analysis

The all-category models showed that skin-tone category was significantly associated with all three CES proximity outcomes: single nearest-neighbor ΔE′, CIEDE2000 ΔE_{00}, and three-nearest-neighbor $\Delta E'_{3NN}$ (Table 3). This pattern was observed across the full five-category skin-tone range. The partial eta-squared values for skin-tone category were large across all three outcomes, indicating that category membership accounted for a substantial portion of the variance in CES proximity. This statistical pattern is consistent with the distributions shown in Figure 2, the category-level mean

 doi:10.20944/preprints202605.2042.v1

trends in Figure 3, the spatial separations shown in Figure 5, and the designated-CES distances summarized in Table 4.

Table 3. ANOVA-style summaries of linear model effects for category-level differences in CES proximity metrics.

Outcome	Effect	F	df	p	η_p^2
ΔE′	Skin-tone category	18.56	4, 90	<0.001	0.45
ΔE′	Dataset	0.30	1, 90	0.586	0.003
ΔE′	Category × dataset	0.47	4, 90	0.756	0.02
ΔE_{00}	Skin-tone category	16.95	4, 90	<0.001	0.43
ΔE_{00}	Dataset	0.18	1, 90	0.673	0.002
ΔE_{00}	Category × dataset	0.40	4, 90	0.808	0.02
$\Delta E'_{3NN}$	Skin-tone category	20.26	4, 90	<0.001	0.47
$\Delta E'_{3NN}$	Dataset	1.70	1, 90	0.196	0.02
$\Delta E'_{3NN}$	Category × dataset	1.92	4, 90	0.114	0.08

The secondary comparison between the Very Light and Very Dark categories illustrated the largest category separation. In the ISSA dataset, Very Dark samples were farther from their nearest CES than Very Light samples [$t(18) = 5.81$, $p < 0.001$, $d = 2.60$]. The same pattern was observed in the CIE dataset [$t(18) = 9.23$, $p < 0.001$, $d = 4.13$]. In the combined dataset, Very Light samples had a mean nearest-neighbor distance of 4.12 ± 0.73 ΔE′, whereas Very Dark samples had a mean distance of 8.04 ± 1.63 ΔE′, corresponding to an approximately 95% increase. This combined contrast was statistically significant [$t(38) = 9.83$, $p < 0.001$, $d = 3.11$].

The 3NN analysis provided a broader structural check on CES proximity. Combined $\Delta E'_{3NN}$ values were 6.03 ± 0.33 for Very Light samples and 9.49 ± 1.90 for Very Dark samples, indicating that the Very Light-to-Very Dark separation was not driven only by the identity of the single closest CES.

Figure 3 summarizes the mean ΔE′ values across categories for both datasets and the combined trend. Nearest-neighbor assignment pattern analysis is reported in the following section.

Table 4. Combined-dataset mean ΔE′ distances from measured skin samples to CES #15 and CES #18, shown separately and as the smaller distance to either designated skin CES.

Category	ΔE′ to CES #15 Mean ± SD	ΔE′ to CES #18 Mean ± SD	Nearest designated skin CES Mean ± SD	Nearest designated CES count*
Very Light	4.62 ± 1.05	19.32 ± 0.97	4.62 ± 1.05	#15: 20, #18: 0
Light	5.21 ± 1.77	11.01 ± 2.16	5.21 ± 1.77	#15: 20, #18: 0
Medium	14.01 ± 5.02	5.20 ± 2.41	5.06 ± 2.21	#15: 3, #18: 17
Dark	26.71 ± 2.85	11.77 ± 3.00	11.77 ± 3.00	#15: 0, #18: 20
Very Dark	36.62 ± 2.74	22.07 ± 2.93	22.07 ± 2.93	#15: 0, #18: 20

* Reports the number of samples, out of 20 per category, for which each skin-designated CES was nearer.

 doi:10.20944/preprints202605.2042.v1

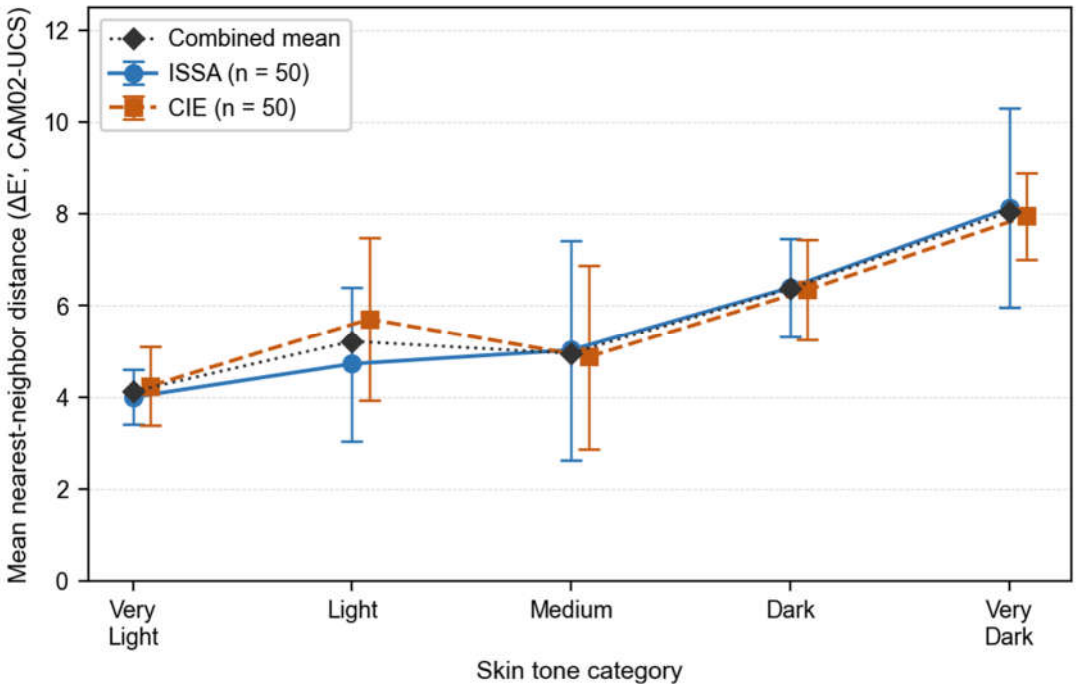

Figure 3. ΔE' difference by skin tone category across datasets.

3.4. CES Utilization Patterns and Designated Skin-CES Distances

Nearest-neighbor assignments were concentrated among a small subset of the TM-30 CES (Figure 4). Across the combined dataset, CES #15 was the most frequent nearest neighbor, accounting for 36 of 100 samples. CES #13 accounted for 16 samples, CES #18 for 15 samples, CES #3 for 10 samples, CES #14 for 7 samples, CES #16 for 6 samples, CES #9 for 5 samples, CES #17 for 4 samples, and CES #39 for 1 sample. The three most frequently assigned CES, #15, #13, and #18, accounted for 67% of all nearest-neighbor assignments.

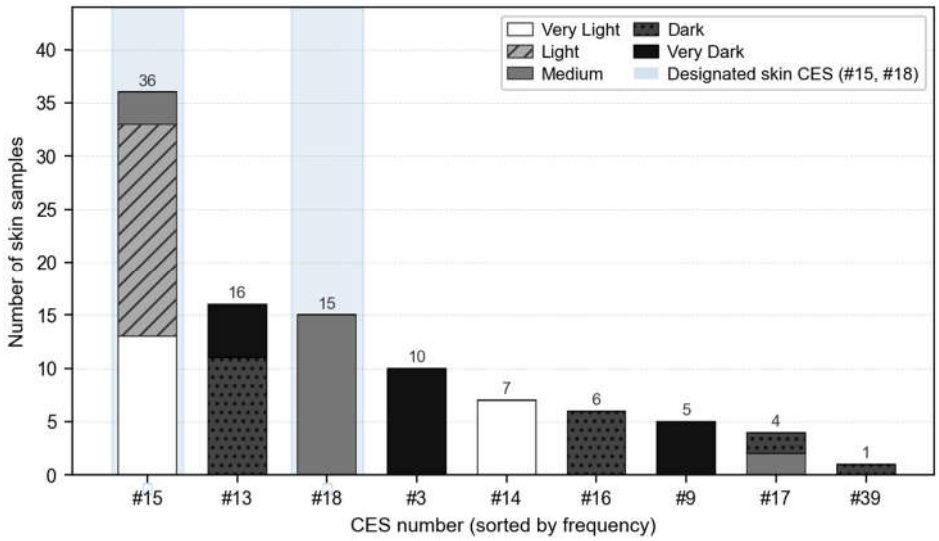

Figure 4. Nearest-neighbor CES usage frequency across skin tone categories.

Only CES #15 and CES #18 are designated skin-tone samples in TM-30-24 and their respective colorimetric coordinates provide context for this assignment pattern. Under D65 using the CIE 1964 10° observer, CES #15 has $L^* = 66.75$, $a^* = 10.85$, and $b^* = 15.19$, while CES #18 has $L^* = 51.66$, $a^* = 10.61$, and $b^* = 19.59$. Both samples lie in the yellow-red region of color space, but their lightness values

 doi:10.20944/preprints202605.2042.v1

correspond primarily to the Light and Medium portions of the skin-tone range used in this study. This is consistent with their frequent nearest-neighbor assignments among Very Light, Light, and Medium samples, and with the tendency of Dark and Very Dark samples to map to other nearby CES. Direct distances to CES #15 and CES #18 further clarifies the role of the designated skin CES.

The distances were examined separately for the two CES and summarized as the smaller distance to either. CES #15 was nearest to all Very Light and Light samples, whereas CES #18 was nearest to most Medium samples and all Dark and Very Dark samples. However, the distance to the nearest designated skin CES increased substantially for Dark and Very Dark samples, indicating that the designated skin CES are positioned closest to the lighter-to-medium portion of the measured skin-tone range (Table 4). It must be noted that the final column in Table 4 should be interpreted only within the two-sample designated skin CES subset. Although CES #18 was the nearer of the two designated skin CES for all Dark and Very Dark samples, these categories more often mapped to non-designated CES as their overall nearest neighbor when all 99 CES were considered.

When all 99 CES were considered, CES #15 and CES #18 were the nearest neighbors for 51 of the 100 skin samples, with assignments concentrated primarily in the Very Light, Light, and Medium categories. Dark and Very Dark samples more often mapped to 'non-skin' CES, particularly CES #13, #3, #9, and #16. Note that this differs from the designated-CES-only comparison in Table 4, where CES #18 was the nearer of the two designated skin CES for darker samples but remained relatively distant in absolute CAM02-UCS terms. This pattern describes the local distribution of the CES relative to measured skin-tone locations; it does not imply that the non-designated CES are inappropriate within TM-30's broader object-color sample set.

Figure 5 shows the spatial relationship between the measured skin samples and the TM-30 CES in CAM02-UCS. Skin samples occupy the expected reddish-yellow region of color space, while nearest-neighbor connector lines show larger separations for darker samples, particularly along the lightness dimension. This visualization is consistent with the category-level distance results reported in Tables 1 and 2 and with the broader model results in Table 3. It also provides spatial context for the designated-CES analysis in Table 4, where distances to CES #15 and CES #18 increase for Dark and Very Dark samples.

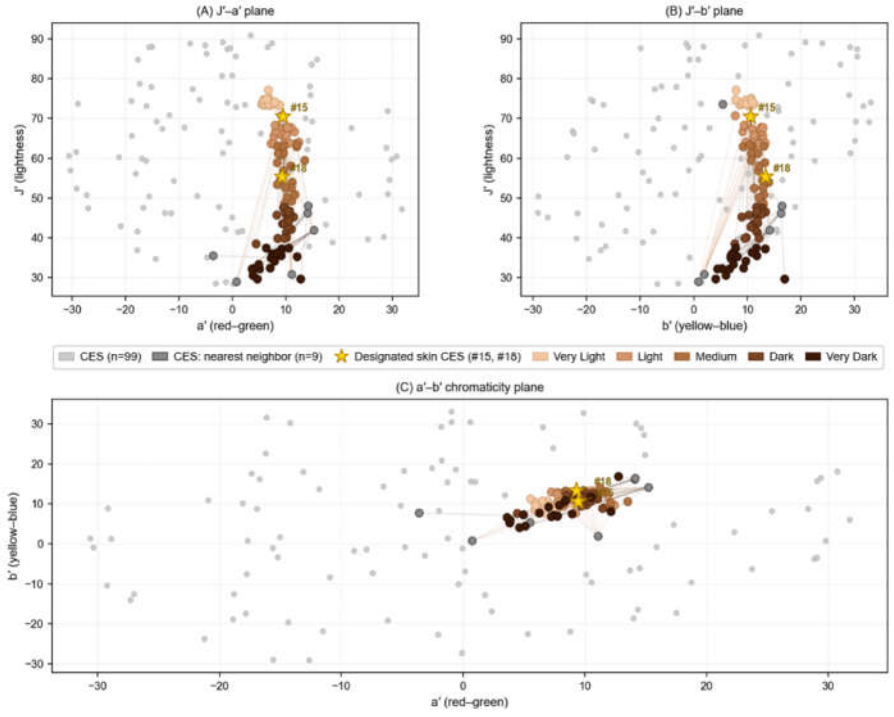

Figure 5. Spatial distribution of measured skin-tone samples and TM-30-24 CES in CAM02-UCS color space. (A) J′–a′ plane. (B) J′–b′ plane. (C) a′–b′ chromaticity plane. Connector lines indicate each skin sample's nearest CES.

 doi:10.20944/preprints202605.2042.v1

4. Discussion

This document discusses how measured human skin tones are positioned relative to the ANSI/IES TM-30-24 CES set. Across two independent datasets, skin-tone category was significantly associated with CES proximity across CAM02-UCS nearest-neighbor distance, CIEDE2000 distance, and mean three-nearest-neighbor distance. The Very Dark category showed substantially larger nearest-CES distances than the Very Light category, with some variability among intermediate categories. In the combined dataset, Very Dark samples were approximately 95% farther from their nearest CES than Very Light samples. The 3NN analysis further supported this interpretation, indicating that the pattern was not driven only by the identity of the single closest CES. Together, these results are best interpreted as a colorimetric sampling-density pattern within a localized region of color space. The TM-30 CES were developed to support general color rendition evaluation across a broad range of object colors encountered in built environments, not to function as a skin-tone database (David et al., 2015; ANSI/IES TM-30-24, 2024). The present analysis narrows attention to one visually important subset of colors and shows that local CES proximity within that subset varies with skin-tone lightness.

The CES utilization results provide further context for this pattern with two CES (#15 and #18) designated as skin-tone samples in TM-30-24 serving as nearest neighbors for 51 of the 100 measured skin samples, primarily in the Very Light, Light, and Medium categories. The direct distance analysis to the two skin-designated CES showed that CES #15 was closest to the Very Light and Light categories, whereas CES #18 was closest to most Medium samples and all Dark and Very Dark samples. However, the distance to CES #18 also increased substantially for the darker categories, indicating that the designated skin CES are most proximate to the lighter-to-medium portion of the measured skin-tone range. This should be read as a structural observation about the position of measured skin tones relative to the CES set. It does not imply that 'non-skin' CES are inappropriate within TM-30's intended gamut-wide sample set, nor does it suggest that the current CES set was expected to span the skin-tone locus with equal local density. The result clarifies where the two designated skin CES sit relative to a broader set of measured skin reflectance spectra.

Several limitations should guide interpretation of these findings. First, the analysis used 100 selected skin reflectance spectra from two datasets, with balanced sampling across lightness categories. This design supports category-level comparison but does not estimate population prevalence or the full distribution of human skin reflectance. The focus on facial measurement sites was intentional, given the relevance of face appearance in built-environment lighting, but the results should not be generalized to all body sites without further analysis. Second, the L^*-based categories are analytical bins rather than fixed biological or demographic classes. Skin color varies continuously across individuals and body sites, and other classification systems may define categories differently. Third, nearest-neighbor distance in CAM02-UCS describes colorimetric proximity under D65, not spectral similarity or rendering fidelity under test illuminants. The 3NN analysis reduces dependence on a single closest CES and supports the interpretation of a local structural pattern, but both nearest-neighbor approaches remain geometric measures of proximity instead of complete spatial-density models. The CIEDE2000 analysis provides a useful robustness check because ΔE_{00} has stronger perceptual grounding than the original CIELAB ΔE_{ab}^*, but it does not substitute for psychophysical validation of skin appearance under real or simulated light sources (Luo et al., 2001; He et al., 2022). Two samples that are close in color space under a reference illuminant may have different spectral reflectance functions and may respond differently under spectrally complex light sources. Finally, the analysis treats skin samples as isolated reflectance spectra, whereas real-world skin appearance is affected by spatial variation, texture, geometry, observer adaptation, and viewing context (Fairchild, 2013; Kiritani et al., 2017). These limitations define the scope of the result: the study characterizes CES sampling density relative to measured skin tones, not perceptual adequacy or lighting performance.

The findings nevertheless point to a useful direction for supplementary skin-specific analyses. TM-30 should remain the general color rendition framework, with R_f, R_g, and related measures

 doi:10.20944/preprints202605.2042.v1

describing broad color fidelity and gamut behavior. For applications in which skin appearance is especially important, such as healthcare, cosmetics, hospitality, retail, residential, and other people-centered environments, additional analyses based on measured skin reflectance spectra may provide more targeted information. Such analyses could be reported alongside standard TM-30 metrics rather than replacing them. A skin-specific descriptor, for example, could evaluate a broader set of measured skin spectra under test and reference illuminants, while preserving TM-30's general-purpose role. The study provides the colorimetric basis for that work by identifying how measured skin tones are positioned relative to the TM-30 CES set and to the two designated skin CES. A companion metric-level analysis can test whether these sampling-density patterns translate into differences in calculated color rendition across practical LED spectra. Until such evidence is available, the present findings should be treated as a map of CES sampling density in the skin-tone region, not as a direct assessment of skin-tone rendering quality.

5. Conclusions

This manuscript discussed how measured human skin tones are positioned relative to the ANSI/IES TM-30-24 Color Evaluation Sample set. Using 100 skin reflectance spectra from the ISSA and CIE datasets, nearest-neighbor distances were calculated in CAM02-UCS under D65 and compared across five skin-tone lightness categories. The results showed a consistent primary contrast across both datasets: Very Dark samples were farther from their nearest CES than Very Light samples. In the combined dataset, Very Dark samples had a mean nearest-neighbor distance of 8.04 ± 1.63 $\Delta E'$, compared with 4.12 ± 0.73 $\Delta E'$ for Very Light samples, corresponding to an approximately 95% increase.

The CES utilization results further showed that the two designated skin-tone samples in TM-30-24, CES #15 and CES #18, served as nearest neighbors for 51 of the 100 measured skin samples, primarily in the Very Light, Light, and Medium categories. Darker skin-tone categories more often mapped to CES without skin designation. This pattern should be interpreted as a local colorimetric sampling result, not as a direct measure of rendering fidelity, spectral similarity, or perceptual adequacy. The all-category and designated-CES analyses show that this pattern is not only an extreme-category contrast, but also a structural feature of how the measured skin-tone region relates to the TM-30 CES set and to CES #15 and CES #18 specifically.

The findings support the value of supplementary skin-specific analyses for applications in which skin appearance is an important lighting consideration. Such analyses would complement TM-30's general color rendition framework. Future work should also test whether the sampling-density patterns identified here translate into meaningful differences in calculated or perceived skin-tone rendering under practical light-source spectra.

Funding Details: The authors report no funding.

Disclosure Statement: The authors report there are no competing interests to declare.

Data Availability Statement: Data and analysis code supporting this study are available through the Open Science Framework at https://doi.org/10.17605/OSF.IO/4NCTE. The repository includes processed colorimetric outputs, source-data documentation, sample-selection notes, and scripts used to reproduce the distance calculations, statistical models, and manuscript figures. Source skin reflectance datasets are subject to the redistribution terms of the original data providers.

References

ANSI/IES. 2024. ANSI/IES TM-30-24. New York, N.Y.: Illuminating Engineering Society.

Chardon A, Cretois I, Hourseau C. 1991. Skin colour typology and suntanning pathways. International Journal of Cosmetic Science. 13(4):191–208. https://doi.org/10.1111/j.1467-2494.1991.tb00561.x

 doi:10.20944/preprints202605.2042.v1

David A, Fini PT, Houser KW, Ohno Y, Royer MP, Smet KAG, Wei M, Whitehead L. 2015. Development of the IES method for evaluating the color rendition of light sources. Opt Express, OE. 23(12):15888–15906. https://doi.org/10.1364/OE.23.015888

Del Bino S, Duval C, Bernerd F, Bino SD, Duval C, Bernerd F. 2018. Clinical and Biological Characterization of Skin Pigmentation Diversity and Its Consequences on UV Impact. International Journal of Molecular Sciences [Internet]. [accessed 2025 Dec 6] 19(9). https://doi.org/10.3390/ijms19092668

Fairchild MD. 2013. Color Appearance Models. 3rd ed. Sussex: John Wiley & Sons. https://doi.org/10.1002/9781118653128

He J, Lin Y, Yano T, Noguchi H, Yamaguchi S, Matsubayashi Y. 2017. Preference for appearance of Chinese complexion under different lighting. Lighting Research & Technology. 49(2):228–242. https://doi.org/10.1177/1477153515615171

He R, Xiao K, Pointer M, Bressler Y, Liu Z, Lu Y. 2022. Development of an image-based measurement system for human facial skin colour. Color Research & Application. 47(2):288–300. https://doi.org/10.1002/col.22737

Jablonski NG, Chaplin G. 2017. The colours of humanity: the evolution of pigmentation in the human lineage. Philos Trans R Soc Lond B Biol Sci. 372(1724):20160349. https://doi.org/10.1098/rstb.2016.0349

Kiritani Y, Komuro Y, Okazaki A, Takano R, Ookubo N. 2017. Assimilation Effects of Eye Shadow on Facial Colors. Japanese Psychological Research. 59(4):288–300. https://doi.org/10.1111/jpr.12164

Lu Y, Xiao K, Pointer M, He R, Zhou S, Nasseraldin A, Sueeprasan S, Gao C, Li C, Sohaib A, et al. 2025. The International Skin Spectra Archive (ISSA): a multicultural human skin phenotype and colour spectra collection. Sci Data. 12(1):487. https://doi.org/10.1038/s41597-025-04857-5

Luo MR, Cui G, Li C. 2006. Uniform colour spaces based on CIECAM02 colour appearance model. Color Research & Application. 31(4):320–330. https://doi.org/10.1002/col.20227

Luo MR, Cui G, Rigg B. 2001. The development of the CIE 2000 colour-difference formula: CIEDE2000. Color Research & Application. 26(5):340–350. https://doi.org/10.1002/col.1049

Okuda S, Okajima K. 2019. PREFERABLE LIGHTING FOR APPEARANCE OF WOMEN'S FACIAL SKIN. PROCEEDINGS OF the 29th Quadrennial Session of the CIE.:1503–1506. https://doi.org/10.25039/x46.2019.po147

Veitch JA, Whitehead LA, Mossman M, Pilditch TD. 2014. Chromaticity-matched but spectrally different light source effects on simple and complex color judgments. Color Research & Application. 39(3):263–274. https://doi.org/10.1002/col.21811

Weatherall IL, Coombs BD. 1992. Skin Color Measurements in Terms of CIELAB Color Space Values. Journal of Investigative Dermatology. 99(4):468–473. https://doi.org/10.1111/1523-1747.ep12616156

Xiao K, Yates JM, Zardawi F, Sueeprasan S, Liao N, Gill L, Li C, Wuerger S. 2017. Characterising the variations in ethnic skin colours: a new calibrated data base for human skin. Skin Research and Technology. 23(1):21–29. https://doi.org/10.1111/srt.12295

Yano T, Hashimoto K. 2016. Preference index for Japanese complexion under illuminations. Color Research & Application. 41(2):143–153. https://doi.org/10.1002/col.21948

Zonios G, Bykowski J, Kollias N. 2001. Skin Melanin, Hemoglobin, and Light Scattering Properties can be Quantitatively Assessed In Vivo Using Diffuse Reflectance Spectroscopy. Journal of Investigative Dermatology. 117(6):1452–1457. https://doi.org/10.1046/j.0022-202x.2001.01577.x